Journal of Photochemistry and Photobiology A: Chemistry 202 (2009) 115–121

Contents lists available at ScienceDirect

Journal of Photochemistry and Photobiology A: Chemistry

journal homepage: www.elsevier.com/locate/jphotochem

Synthesis and photochemical reaction of novel, visible-wavelength oxidizable polymerization sensitizer based on the 12H-quinoxalino[2,3-b][1,4]benzothiazine skeleton

Radosław Podsiadły*

Institute of Polymer and Dye Technology, Technical University of Lodz, Stefanowskiego 12/16, 90-924 Lodz, Poland

ARTICLE INFO

Article history:
Received 3 October 2008
Received in revised form
26 November 2008
Accepted 29 November 2008
Available online 11 December 2008

Keywords:
12H-quinoxalino[2,3-b][1,4]benzothiazine dyes
Sensitized free radical polymerization
Photoinduced electron transfer

ABSTRACT

Novel dyes based on the 12H-quinoxalino[2,3-b] [1,4]benzothiazine skeleton were synthesized and subsequently characterized using ^{1}H NMR. Their electrochemical and spectral properties, such as absorption and emission spectra, quantum yield of fluorescence, and quantum yield of singlet oxygen formation, were measured. These compounds were evaluated as sensitizers for alkoxypyridinium salt photodecomposition, and the results are discussed on the basis of the free energy change for electron transfer from benzothiazine dyes to alkoxypyridinium compounds. Benzothiazine dyes are useful oxidizable sensitizers for *N*-alkoxypyridinium photoinitiators. The mechanism of the dye photobleaching is supported by time-dependent density functional theory (TD-DFT) calculations and the quantum yields of sensitized proton formation. Photoredox pairs consisting of benzothiazine dyes and alkoxypyridinium salt were found to be effective initiation systems for free radical polymerization of methyl acrylate and trimethylolpropane triacrylate (TMPTA) using visible light.

1. Introduction

Light-induced photopolymerization has several advantages over other methods. The process occurs at low temperatures and can be controlled by manipulating the intensity and wavelength irradiation. Photoinitiated free radical polymerization of multifunctional monomers produces highly crosslinked polymers with high thermal stability, mechanical strength, and resistance to solvent. Therefore, these polymers have many industrial applications, especially in coatings for flooring and furniture, dental restorative materials, optical fibre coatings, hard and soft contact lenses and photolithography [1,2].

Many early photoinitiating systems for free radical polymerization were sensitive to UV light. In free radical photopolymerization, the UV-absorbing compounds undergo direct fragmentation in excited states to form the initiating radicals, as shown in Scheme 1 for the *N*-alkoxypyridinium compound [3].

A sensitizer was used to extend the spectral sensitivity to visible light. The photoinduced intermolecular electron transfer (PET) yields free radicals that initiate polymerization. The mechanism for the pyridinium salt is shown in Scheme 2 [3]. In oxidizable sensitization, the excited sensitizer (Dye^*) is oxidized by the pyridinium salt to form the corresponding radical cation ($Dye^{\bullet+}$) and onium salt radical. The rapid decomposition of the pyridinium radical into pyridine and an alkoxy radical retards the back electron transfer and renders the overall process irreversible.

The visible photoinitiators operating via oxidizable sensitization are very rare, with only cyanine [4], coumarin [5], acridinedione dyes [6] and fluoflavin dyes [7] initiating acrylate monomer photopolymerization via electron transfer from the excited states of the dyes to onium salts.

In oxidizable sensitization, the sensitizer should have a low ionization potential. Therefore, the phenothiazine derivatives with low oxidation potentials are the best compounds [8], and they are applied as sensitizers for radical polymerization [3]. Unfortunately, phenothiazines absorb below 400 nm. The main goals of this study were to synthesize novel sensitizers based on the 12H-quinoxalino-[2,3-b][1,4]-benzothiazine (**4a**–**4c**) skeleton and to evaluate these dyes' spectroscopic, photophysical, and electrochemical properties. This paper reports the photochemical properties of pyridinium (**Py1**-**Py2**)/benzothiazine dye systems, in particular the photobleaching of the dye. The mechanism of dye fading proposed here is supported by time-dependent density functional theory calculations (TD-DFT), spectroscopic characterization of products formed during photolysis of the dye/onium salt system and the quantum yields of sensitized proton formation. Finally, it was demonstrated that these new photooxidizable sensitization systems can be used as visible photoinitiators for free radical polymerization of acrylate monomers.

* Tel.: +48 42 631 3237; fax: +48 42 636 25 96.
E-mail address: radekpod@p.lodz.pl.

1010-6030/$ – see front matter © 2008 Elsevier B.V. All rights reserved.
doi:10.1016/j.jphotochem.2008.11.017

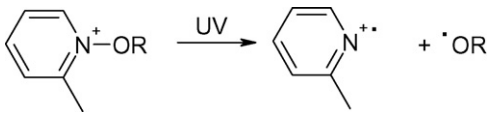

Scheme 1. .

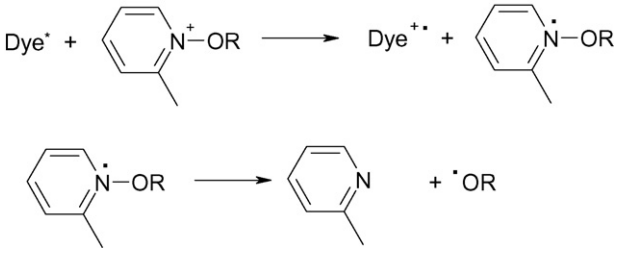

Scheme 2. .

2. Experimental

2.1. General

Synthesis reagents and *N*-methoxy-4-phenylpyridinium tetrafluoroborate (**Py1**) were purchased from Aldrich (Poznan, Poland). *N*-ethoxy-2-methylpyridinium hexafluorophosphate (**Py2**) was synthesized as described in Ref. [7]. The final products were identified by ^{1}H NMR spectroscopy [Bruker Avance DPX 250, DMSO-d_6, TMS standard, δ (ppm)]. Their purity was checked through TLC [Merck Silica gel 60 solvent toluene:ethyl acetate 4:1 (v/v)]. The absorption and steady-state fluorescence spectra were recorded using a Lambda 40 spectrophotometer (PerkinElmer, USA) and a FluoroLog 3 spectrofluorimeter (Jobin Yvon-Spex, USA), respectively.

2.2. Synthesis

2.2.1. Synthesis of 1,4-dihydroquinoxaline-2,3-dione **2a**

Ortho-phenylenediamine (4.32 g, 0.04 mol) and oxalic acid (5.04 g, 0.04 mol) were refluxed in hydrochloric acid (40 ml, 30%) for 3 h. After cooling, the gray precipitate was filtered, washed with water, dried and used in the next step without further purification. The product (5.36 g) was obtained with an 82% yield (m.p. 298 °C (300 °C [9])). The other dihydroquinoxaline-2,3-diones (**2b**, **2c**) were synthesized in the same way using the appropriate *ortho*-phenylenediamines. The yields and melting points of these compounds are presented in Table 1.

2.2.2. Synthesis of 2,3-dichloroquinoxaline **3a** [10]

Dimethylformamide was added dropwise (0.1 ml) to a solution of **2a** (4.0 g, 0.025 mol) in thionyl chloride (120 ml). The reaction mixture was refluxed for 10 h and then concentrated under vacuum. The resulting residue was co-evaporated with chloroform several times, dissolved in chloroform (100 ml), and poured onto ice water. The organic layer was collected, washed with saturated aqueous NaCl, dried over $MgSO_4$, and then evaporated to provide **3a** as a cream solid (4.26 g, 87%, m.p. 148–150 °C (149 °C [11])), which was used without further purification in the next step. The dichloroquinoxalines **3b** and **3c** were synthesized in the same way using the appropriate substrates **2b** and **2c**, respectively. The yields and melting points of these compounds are presented in Table 1.

Table 1
Yields and melting points of the quinoxalines **2** and **3**.

	Yield (%)	m.p. (°C)
2a	82	298 (300 [9])
2b	64	304–307
2c	89	>360 (>360 [13])
3a	87	148–150 (149 [11])
3b	87	182 (183 [14])
3c	74	173 (173–174 [13])

2.2.3. Synthesis of 12H-quinoxalino[2,3-b][1,4]benzothiazine **4a** [12]

2,3-dichloroquinoxaline (2.20 g, 0.011 mol), *ortho*-aminothiophenol (1.38 g, 0.011 mol) and Na_2CO_3 (3.30 g, 0.011 mol) were refluxed in *ortho*-dichlorobenzene (40 ml) for 1 h. After cooling, the orange precipitate was filtered, washed with methanol, dried and recrystallized from acetic acid. The product (1.97 g) was obtained with a 71% yield. The other dyes were synthesized in the same way using the appropriate dichloroquinoxalines. The yield, melting point, R_f and ^{1}H NMR data for all synthesized dyes are presented in Table 2.

2.3. Photochemical experiments

All photochemical experiments were carried out in a Rayonet Reactor RPR 200 (Southern New England Ultraviolet Co., USA) equipped with eight lamps emitting light at 419 nm. Illumination intensity was measured using uranyl oxalate actinometry [15].

Photodecomposition of **Py1** (0.1 mM, 5 ml) sensitized by benzothiazine dye (0.1 mM) in 1-methyl-2-pyrrolidone was carried out in a glass tube under an N_2 atmosphere. The extent of dye fading was determined according to the decrease in absorption at λ_{max}. The quantum yield of dye bleaching Φ_{bl} was calculated from at least three determinations when the reaction was $10 \pm 3\%$ complete. Photobleaching of the dye (0.1 mM) in solution with **Py2** (0.1 mM, 5 ml) was determined in the same way.

The quantum yield of sensitized proton formation $\Phi(H^+)$, the quantum yield of singlet oxygen formation $\Phi(^1O_2)$, electrochemical experiments and fluorescence lifetime were measured as described in Ref. [7].

The fluorescence quantum yield of the dye (Φ_{dye}) was calculated from the following equation:

$$\Phi_{dye} = \frac{\Phi_{ref} I_{dye} A_{ref} {n_{dye}}^2}{I_{ref} A_{dye} {n_{ref}}^2} \quad (1)$$

where Φ_{ref} denotes the fluorescence quantum yield of the 5,12-dihydroquinoxalino[2,3-b]quinoxaline reference ($\Phi_{ref} = 0.8$ in 1-methyl-2-pyrrolidone [7]), A_{dye} and A_{ref} denote the absorbances of the dye and the reference at the excitation wavelengths (410 nm), I_{dye} and I_{ref} refer to the areas under the fluorescence peaks of the dye and reference, and n_{dye} and n_{ref} are the solvent refractive index for the dye and reference, respectively.

The Stern–Volmer constants were obtained from fluorescence quenching experiments. The fluorescence spectra of dye solutions (15–20 μM) in EtOH containing various amounts of quenchers were measured at room temperature in an air atmosphere using excitation at λ_{max} for **Py1** or **Py2**, respectively. Relative fluorescence intensities (I_0/I) were determined by measuring the heights of the peak at λ_{em}. Free radical photopolymerization was carried out in solutions composed of 1 ml of 1-methyl-2-pyrrolidone and 4 ml of methyl acrylate (MeAc) or trimethylolpropane triacrylate (TMPTA). 1-methyl-2-pyrrolidone was added to improved solubility of the sensitizer. The dye concentration was 0.1 mM, and the concentration of alkoxypyridinium salts was 10 mM. The rate of polymerization (R_p) was calculated using Eq. (2), where Q_s is the heat flow per second during the reaction, m is the mass of the monomer in the sample, M is the molar mass of the monomer, n is the number of double bonds per monomer, and ΔH_p is the theo-

Table 2
Yield, R_f, melting point and ^{1}H NMR data of dyes **4**.

Dye	m.p. (°C)	R_f[a]	Yield (%)	^{1}H NMR DMSO-d_6
4a	281 (282–283 [12])	0.78	71	3.90 (s, 1H), 6.77–6.88 (m, 2H), 7.00–7.09 (m, 2H), 7.27–7.57 (m, 1H), 7.38–7.67 (m, 2H), 7.50–7.54 (m, 1H)
4b	305	0.77	72	2.42 (s, 3H), 2.46 (s, 3H), 6.63–6.71 (m, 1H), 6.86–6.91 (m, 1H), 7.04–7.17 (m, 1H), 7.27–7.35 (m, 1H), 7.37–7.41 (m, 1H), 7.51 (s, 1H), 7.78 (s, 1H)
4c	328	0.78	77	5.90–5.99 (m, 1H), 6.89–6.98 (m, 2H), 7.10–7.16 (m, 2H), 7.64–7.66 (m, 1H), 7.84 (s, 1H)

[a] Merck Silica Gel 60 eluent: toluene:ethyl acetate (4:1) (v/v).

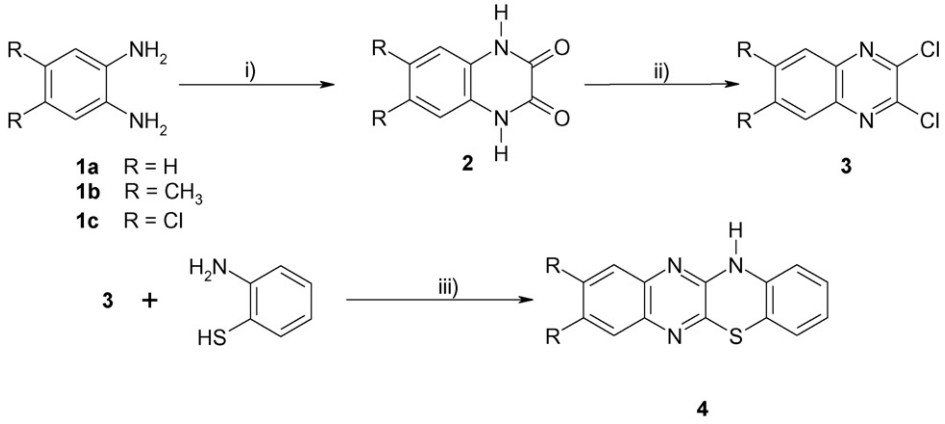

Scheme 3. (i) Oxalic acid, 30% HCl; (ii) $SOCl_2$, DMF; (iii) *ortho*-dichlorobenzene, Na_2CO_3

retical enthalpy for complete conversion of acrylate double bonds (20.6 kcal/mol) [16].

$$R_p = \frac{Q_s \cdot M}{n \cdot \Delta H_p \cdot m} \quad (2)$$

For the detection of the heat flow, a PT 401 temperature sensor (Elmetron, Poland) immersed in the sample was used. The conversion of methyl acrylate into poly(methyl acrylate) after a 2-min irradiation was determined gravimetrically. Each reported R_p and conversion represents the average value of five measurements.

2.4. Quantum chemical calculations

The geometries of all species were optimized by the B3LYP density functional method [17,18] as implemented in the Gaussian 03 suite of programs [19]. The above calculations were done for the ground states with the standard 6-31G* basis set. The optimized structures were characterized by harmonic frequency analysis as local minima (all frequencies real). The calculations for electronic excited states of the molecule were performed by the time-dependent DFT (TD-DFT) method [20] using the B3LYP functional method with the same basis set.

3. Results and discussion

3.1. Synthesis and spectroscopic properties

The synthesis of dye **4** is outlined in Scheme 3. In the first step, the *ortho*-phenylenediamines (**1a**–**1c**) were cyclized with oxalic acid in refluxing hydrochloric acid (30%) to give the appropriate 1,4-dihydroquinoxaline-2,3-diones (**2a**–**2c**), which were then used without further purification in the next step. The chlorination of **2** by treatment with thionyl chloride provided the 2,3-dichloroquinoxaline derivative (**3a**–**3c**) [10]. The yields of these reactions and the melting points of the quinoxaline derivatives **2a**–**2c** and **3a**–**3c** are presented in Table 1. Finally, the dyes **4a**–**4c** were synthesized by the reflux of **3** with *ortho*-aminothiophenol in *ortho*-dichlorobenzene [12]. The crude dyes were purified by recrystallization from acetic acid until a constant molar excitation coefficient and TLC purity were obtained.

The chemical structures of the dyes were verified by ^{1}H NMR (Table 2). The spectroscopic properties (absorption and fluorescence) of dyes **4a**–**4c** are presented in Table 3. The electronic absorption (UV–vis) and emission spectrum of the dye **4a** are presented in Fig. 1. 12H-quinoxalino[2,3-b][1,4]benzothiazine has four

Table 3
Spectroscopic and photophysical parameters of benzothiazine dyes **4** and **BPT**.

Dye	λ_{max}[a] (ε) nm (M^{-1} cm^{-1})	λ_{max}[b] (ε) nm (M^{-1} cm^{-1})	λ_{max}[c] (ε) nm (M^{-1} cm^{-1})	λ_{em}[c] (nm)	SS (nm)	Φ em[c]	τ [c] (ns)	E^* (kJ mol^{-1})	Φ ($^1O_2$)[b]
4a	251 (32,100), 286 (6100), 306 (4860), 359 (4600), 420 (9850)	425 (7400)	421 (6400)	530	109	0.22	4.6	253.5	0.78
4b	252 (30,100), 281 (9460), 306 (6750), 418 (10,100)	426 (7600)	424 (6500)	532	108	0.20	4.3	252.9	0.79
4c	256 (70,300), 287 (6650), 432 (10,800)	442 (7300)	442 (5000)	544	102	0.23	4.1	246.7	0.79
BPT	219, 247, 285, 365 [d]								

[a] CH_2Cl_2.
[b] 1-methyl-2-pyrrolidone.
[c] EtOH.
[d] CH_3CN from Ref. [21].

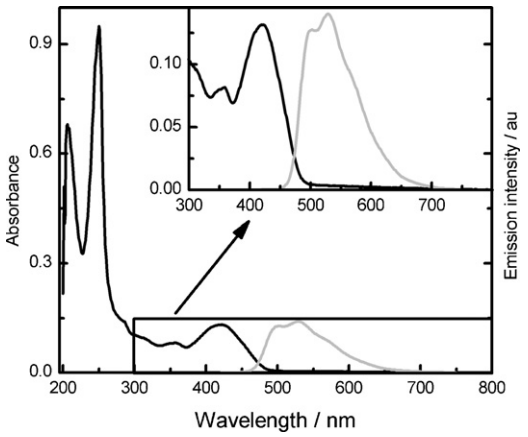

Fig. 1. Normalized absorption (black) and emission (gray) spectra of dye **4a** (15 μM) in EtOH.

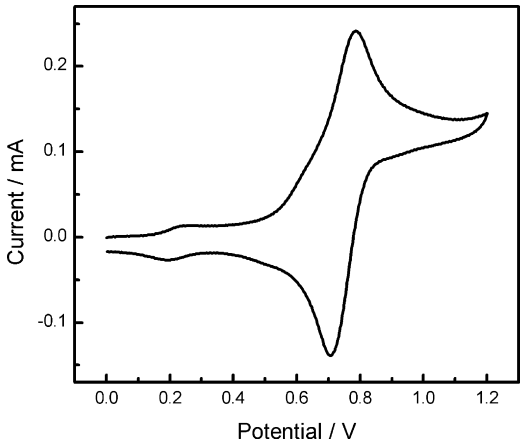

Fig. 2. Cyclic voltammograms of dye **4b** in CH_3CN. Scan rate: 0.1 V s^{-1}.

absorption bands located at 206 nm, 250 nm, 356 nm and 422 nm. In comparison with benzo[b]phenothiazine (**BPT**) [21], the presence of two additional nitrogens in **4a** caused a red shift of the long wavelengths band into the visible region. The position of the visible absorption band depends on the character of the substituents (*R*). The presence of two halogens (**4c**) caused the red shifted absorption band in comparison with spectra from dyes **4a** and **4b**. The examined dyes exhibited moderate solvatochromic effects. A bathochromic shift between a nonpolar (CH_2Cl_2, $\varepsilon = 9.1$) and polar solvent (1-methyl-2-pyrrolidone, $\varepsilon = 33$) of only 5–10 nm was observed.

The studied dyes **4** have an emission band characterized by a Stokes shift of about 102–106 nm. These values indicate that the geometry of the singlet excited state differs from the geometry of the ground state. The fluorescence quantum yield (Φ_{em}) and the lifetime of singlet excited state are presented in Table 3. These data indicate that the singlet lifetime is in the range of 4.1–4.6 ns, and the fluorescence quantum yield of these dyes is in the range of 0.20–0.23. In order to clarify the photochemistry of dyes **4a**–**4c**, the quantum yields of singlet oxygen generation [$\Phi(^1O_2)$] in an oxygen-saturated solution were measured. The ability to generate $^1O_2$ is an indirect confirmation that the photochemical reaction of studied dyes may occur in triplet excited state. The obtained $\Phi(^1O_2)$ are presented in Table 3. These values (~0.8) are comparable with other phenothiazine derivatives that show weak values of quantum yields of fluorescence, but their quantum yields of intersystem crossing are very near one [22].

3.2. Sensitized free radical polymerization

The spectroscopic studies reveal that the dyes **4** can be applied as visible sensitizers for light >400 nm. The well-known mechanism [3] of oxidizable sensitized photodecomposition of alkoxypyridinium salt is presented in Scheme 2. After irradiation, an electron transfer proceeds from the excited sensitizer (Dye*) to pyridinium, followed by the cleavage of the onium radical to give an alkoxy radical, sensitizer radical cation (Dye$^{\bullet+}$) and neutral pyridine.

The free energy change for this photoinduced electron transfer process can be calculated by the Rehm–Weller equation (Eq. (3)) [23]:

$$\Delta G_{et}(\mathrm{kJ\,mol^{-1}}) = 97\left[E_{ox}\left(\frac{S}{S^{\bullet+}}\right) - E_{red}\left(\frac{A^{\bullet-}}{A}\right)\right] - \frac{Ze^2}{\varepsilon a} - E\cdot(s) \qquad (3)$$

In this equation, E_{ox} ($S/S^{\bullet+}$) and E_{red} ($A^{\bullet-}/A$) are the oxidation potential of the dye and the reduction potential of the pyridinium salt, respectively. The $E^*(S)$ is the excited energy state of the dye **4**, as shown in Table 3. In this calculation, the Coulombic energy $Ze^2/\varepsilon a$ was omitted because the dye **4**/pyridinium system is the photoredox pair without an electrostatic interaction in the ground state and after the electron transfer process.

In order to be able to calculate ΔG_{et}, the oxidation potentials of the dyes **4** were measured in separate experiments. The cyclic voltammogram of dye **4b** is presented in Fig. 2, and the measured oxidation potentials (E_{ox}) of all of the dyes are presented in Table 4. In all cases, the oxidation of the dyes is quasi-reversible ($\Delta Ep = E_{ox} - E_{cat} > 0.6$), and the location of the oxidation peak depends on the structure of the dye. The obtained results indicate that the dyes **4** are oxidized at higher potentials in comparison with the most commonly used photosensitizers such as phenothiazine (**PT**) and benzo[b]phenothiazine (**BPT**). Among the studied dyes, compound **4b** is more readily oxidized in comparison with the halogen-substituted analogue **4c** and unsubstituted dye **4a**. This is illustrated by the position of the oxidation peak at 0.79 V for dye **4b** and at 0.97 V and 0.90 V for dye **4a** and **4c**, respectively.

Once the E_{ox} and E^* values of the dyes **4** and the reduction potential of the onium salt were measured, the ΔG_{et} could be calculated using Eq. (3). The calculated thermodynamic parameters listed in Table 5 indicate that the **4b**/Py systems possess the highest ΔG_{et}. Moreover, all combinations of dye/pyridinium systems possess a high driving force, $-\Delta G_{et} > 40\ \mathrm{kJ\,mol^{-1}}$, after exposure to light, which means that the photoelectron transfer processes easily occur through the excited state. On the basis of this calculation, it can be assumed that the pyridinium photodecomposition caused by the studied dyes is initiated by the photoinduced intermolecular electron transfer from dyes to pyridinium salts. The fluorescence of benzothiazine dyes was effectively quenched by the pyridinium salt (Fig. 3), and the absence of any new peak in the emission spectra excludes the exciplex formation. The obtained Stern–Volmer constants (K_{SV}) and calculated singlet quenching constants k_q are summarized in Table 5. The k_q values are close to the diffusion-controlled limit ($k_q \sim 1 \times 10^{10}\ \mathrm{M^{-1}\,s^{-1}}$) but the highest singlet quenching constants were obtained for dye **4c**.

Table 4
Electrochemical properties of phenothiazine compound (**4**, **PT** and **BPT**).

	E_{ox} (V)	E_{cat} (V)	ΔE_p (V)
4a	0.97	0.87	0.10
4b	0.79	0.71	0.08
4c	0.90	0.83	0.07
PT	0.50 (0.69[a])	0.40	0.10
BPT	0.79[a]	0.87[a]	0.08[a]

[a] In CH_3CN vs. Ag/AgCl, from Ref. [21].

Table 5
Thermodynamic data (kJ mol^{-1}), Stern–Volmer (M^{-1}) and singlet quenching (M^{-1} s^{-1}) constants for **4**/Py photoredox pair, quantum yield of acid release (mmol quant^{-1}) and dye photobleaching (mmol quant^{-1}).

	Py1 (E_{red} = −1.025 V)					**Py2** (E_{red} = −1.225 V)				
	ΔG_{el}	K_{SV}	$k_q \times 10^{-10}$	Φ_{bl} [a]	$\Phi(H^+)$ [b]	ΔG_{el}	K_{SV}	$k_q \times 10^{-10}$	Φ_{bl} [a]	$\Phi(H^+)$ [b]
4a	−60.0	112.9	2.4	1.4	2.1	−40.6	114.5	2.5	2.8	1.6
4b	−76.8	120.4	2.8	4.6	3.9	−57.4	121.4	2.8	9.5	8.3
4c	−60.0	147.3	3.6	5.0	4.4	−40.6	145.3	3.5	3.3	2.9

[a] Quantum yield of dye photobleaching; [Py] = 0.1 mM; [dye] = 0.1 mM; determined for 10 ± 3%.
[b] Quantum yield of acid release; [Py] = 0.1 mM; [dye] = 0.1 mM, [BrPhBlue] = 5 μM; determined for 8 ± 3%.

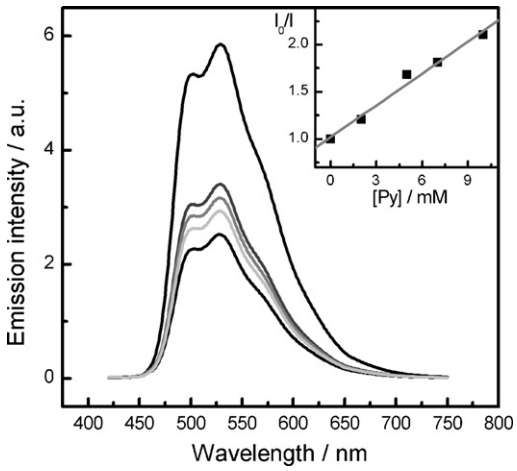

Fig. 3. Fluorescence quenching of dye **4a** by **Py1**. Inset: Stern–Volmer plot of fluorescence quenching of dye **4a** (15 μM) by **Py1** in EtOH.

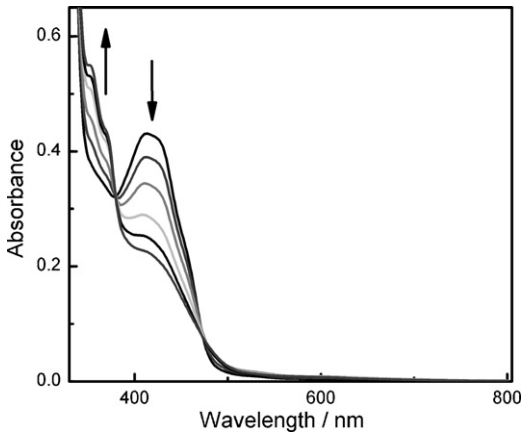

Fig. 4. Electronic absorption spectra obtained upon photolysis of an N_2-saturated solution of a dye **4a** (65 μM)/**Py1** (0.1 mM) system in 1-methyl-2-pyrrolidone (time interval 10 s).

3.3. Dye photobleaching

In the photopolymerization of multifunctional monomers initiated by a dye photoredox pair, the most important properties are high initiation reactivity and photobleaching of the dye. The photobleaching of the dyes **4a**–**4c** was measured in a 1-methyl-2-pyrrolidone solution under an N_2 atmosphere. The photobleaching quantum yields of the dyes (Φ_{bl}) are presented in Table 5. These data clearly indicate that the photobleaching quantum yield depends on the pyridinium salt and the highest Φ_{bl} is obtained for the **4b**/**Py2** photoredox pair.

The absorption spectra of the dye **4a**/**Py1** combination before and during irradiation under an N_2 atmosphere (60–180 s) are shown in Fig. 4. The decay of the dye absorption (427 nm) is accompanied by the growth of the bands around 376 nm and 490 nm. The same effect was observed during photolysis of the dye/**Py2** systems. The isosbestic points (Fig. 4) indicate direct conversion of the dye to the product, which is very stable.

It is well known that the cation radical of sensitizers may react with the alkoxy radical formed during decomposition of pyridinium radical [7,24]. These cationic species undergo deprotonation, releasing the acid (Scheme 5). In the present study, the quantum yield of acid release [$\Phi(H^+)$] in the solution upon photolysis was measured using sodium bromophenol blue (**BPhBl**, Scheme 4). Its absorption at the peak wavelength of 606 nm decreased during irradiation (Fig. 5). The amount of acid release was estimated from the calibration curve of **BPhBl** (inset in Fig. 5). In all of the studied dye/pyridinium combinations, the solution acidity increased, whereas the photolysis of the dyes alone did not change the solution pH.

The calculated quantum yields of acid release are presented in Table 5. The highest Φ (H^+) was obtained during photolysis of **4b**/**Py2** systems. Moreover, in all cases, the Φ (H^+) values were comparable with Φ_{bl}, which suggests that protons are formed in the reaction of the dyes discoloration. It is known [7] that the substitution of the alkoxy radical into the benzene ring in fluoflavin dyes caused a small red-shift absorption in comparison with the parent dye. One can conclude that the reaction of •OR with the cation radical of the benzothiazine dyes should occur in 12 position (Scheme 5). TD-DFT calculations at the B3LYP/6-31G* level reveal that *N*-methoxy dyes show an absorption band in the same wavelength as the product formed during photolysis (Table 6). Moreover,

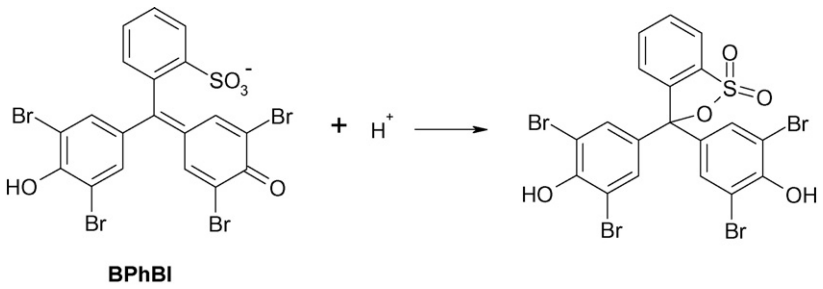

BPhBl

Scheme 4. .

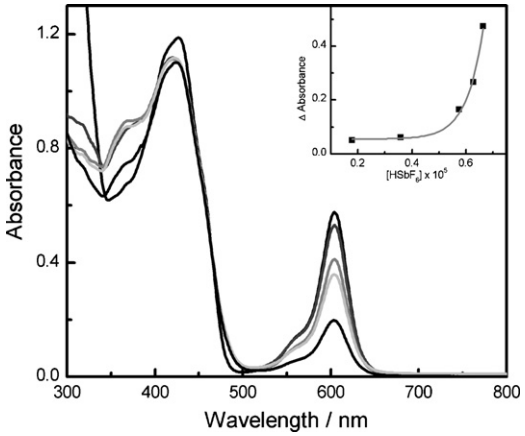

Fig. 5. Electronic absorption spectra obtained upon photolysis (time interval 600 s) of an N_2-saturated solution of **BPhBI** (5 μM) and a dye **4b** (0.1 mM)/**Py1** (0.1 mM) system in 1-methyl-2-pyrrolidone. Inset: calibration curve of **BPhBI** (5 μM) in an $HSbF_6$ solution (concentration range 0–70 μM).

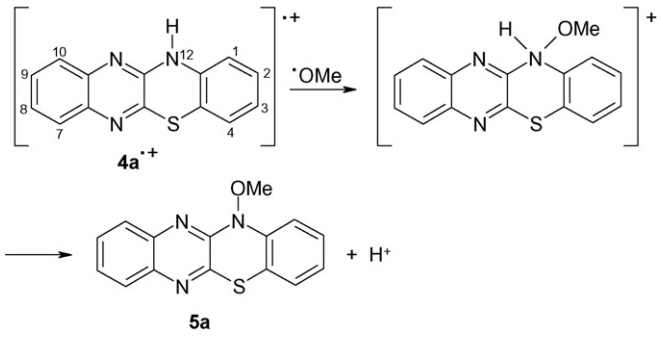

Scheme 5. .

Table 6
Comparison of calculated and experimental absorption maxima for *N*-methoxy derivative **5**.

	λ (nm)	λ calc (f_{osc}) (nm)
5a	490 (sh), 359	379.65 (0.2271), 324.94 (0.0126), 311.81 (0.0044), 304.05 (0.0207), 280.59 (0.0111), 274.64 (0.0185)
5b	495 (sh), 370	379.66 (0.2690), 325.95 (0.0110), 310.27 (0.0064), 305.84 (0.0244), 282.52 (0.0176), 275.45 (0.0098)
5c	510 (sh), 383	396.16 (0.2911), 334.40 (0.0213), 313.25 (0.0189), 312.04 (0.0115), 284.09 (0.0011), 280.75 (0.0026)

the formation of this product was confirmed by the disappearance of the characteristic vibration of the N–H bond at 3050 cm^{-1} in the infrared spectrum obtained after a 5-min irradiation of the **4a**/**Py1** photoredox pair.

On the basis of the results presented above, Scheme 6 proposes a mechanism for how photobleaching of benzothiazine dyes composed of pyridinium salts occurs during photolysis. Scheme uses the system of dye **4a** and **Py2** as an example. The electron transfer proceeds from the excited dye to the pyridinium salt (**Py2**), followed by cleavage of the ethoxypiridinium radical (**Py2•**) to give an ethoxy radical (•OEt), neutral pyridine, and dye radical cation (**4a•+**). The benzothiazine cation radical may react with the ethoxy radical (•OEt) yielding a cation, followed by a proton release and formation of an N-ethoxy derivative of the benzothiazine dye **5a**.

3.4. Photopolymerization

Finally, the usefulness of the benzothiazine-sensitized Py photodecomposition system as the initiator for free radical polymerization of a methyl acrylate (MeAc) and trimethylolpropane

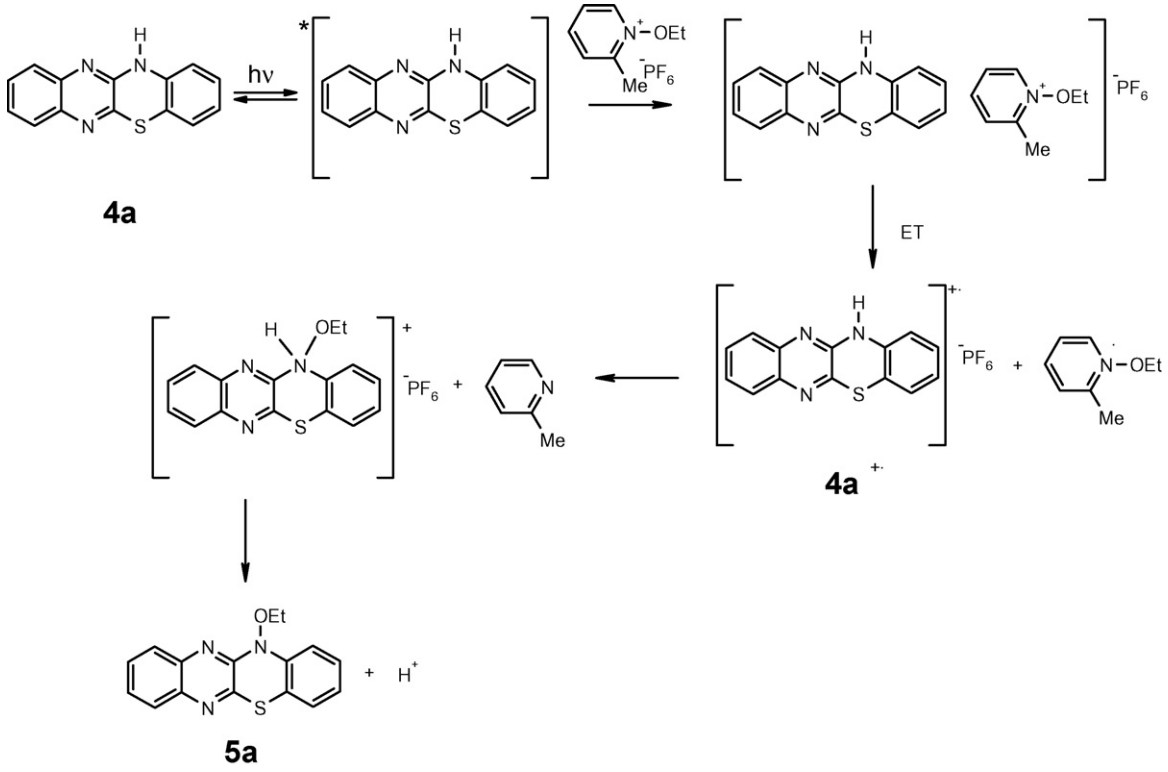

Scheme 6. .

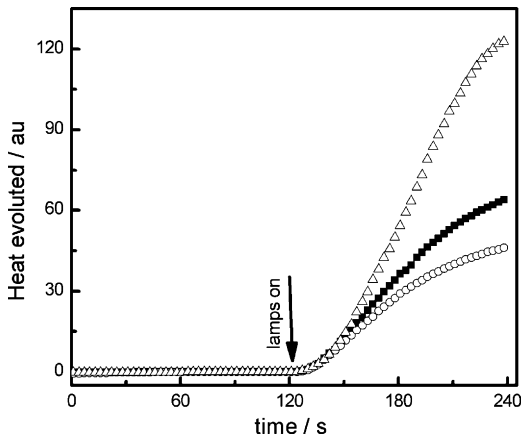

Fig. 6. Photopolymerization kinetic curves of TMPTA recorded for dyes **4a** (■); **4b** (△); **4c** (○) and **Py1**.

Table 7
Rate of polymerization (μmol s^{-1}) and conversion (%) of the monomer in the polymerization initiated by the **4**/Py system.

	Py1			Py2		
	TMPTA	MeAc		TMPTA	MeAc	
	R_p	R_p	Conversion	R_p	R_p	Conversion
4a	17.4	28.1	29	24.4	33.8	22
4b	25.8	32.2	28	33.2	39.6	20
4c	15.2	29.8	27	23.6	28.9	20

triacrylate monomer was examined. The efficiency of the polymerization initiated by the **4**/Py systems was evaluated on the basis of heat flow during the irradiation (Fig. 6). For MeAc, the conversion of the monomer into polymer was also determined after the irradiation, and these results are summarized in Table 7.

Fig. 6 and the calculated polymerization rate (Table 7) indicate that the photoredox pairs consisting benzothiazine dyes **4a**–**4c** as sensitizers and Py as initiators are promising visible systems for initiate the photopolymerization of the acrylate and triacrylate monomer. Among the studied dyes **4**, the most efficient sensitizer is dye **4b** which is oxidized at the lowest potential and therefore **4b**/Py systems possess the highest $-\Delta G_{et}$.

4. Conclusions

Novel dyes based on the 12H-quinoxalino[2,3-b][1,4]benzothiazine skeleton (**4a**–**4c**) were successfully synthesized and characterized using ^{1}H NMR spectroscopy. Benzothiazine dyes sensitize *N*-alkoxypyridinium salts to photodecomposition through electron transfer. The photolysis of a dye/pyridinium system in an N_2 atmosphere yields *N*-alkoxy dyes and a proton. The benzothiazine dyes **4a**–**4c**, when combined with pyridinium salts, may have practical applications as visible-light photoinitiators of free radical polymerization of acrylate monomers.

Acknowledgements

This work was supported by the Polish Ministry of Science and Higher Education (Project No. N N205 1454 33).

References

[1] C. Lowe, G. Webster, S. Kessel, I. McDonald, Chemistry and Technology of UV and EB Formulation for Coatings, Inks and Paints Surface Coating Technology, vol. 4, Wiley, London, 1996.
[2] P.K.T. Oldring, Chemistry and Technology of UV and EB formulation for Coatings, Inks and Paints. Speciality Finishes, vol. 5, Wiley – Sita Techn. Ltd., London, 1997.
[3] W. Schnabel, Macromol. Rapid Commun. 21 (2000) 628–642.
[4] I.R. Gould, D. Shukla, D. Giesen, S. Farid, Helv. Chim. Acta 84 (2001) 2796–2812.
[5] H.J. Timpe, K.P. Kronfeld, U. Lannel, J.P. Fouassier, D.J. Lougnot, J. Photochem. Photobiol. A: Chem. 52 (1990) 111–122.
[6] H.J. Timpe, S. Urlich, J.P. Fouassier, Macromolecules 26 (1993) 4560–4566.
[7] R. Podsiadły, J. Photochem. Photobiol. A: Chem. 198 (2008) 60–68.
[8] S. Nath, H. Pal, D.K. Palit, A.V. Sapre, J.P. Mittal, J. Phys. Chem. A 102 (1998) 5822–5830.
[9] A.H.E. Elwahy, Tetrahedron 56 (2000) 897–907.
[10] J. Ohmami, S. Maso, J. Med. Chem. 40 (1997) 2053–2063.
[11] R. Kuhn, P. Skrabal, P.H.H. Fischer, Tetrahedron 24 (1968) 1843–1894.
[12] S.D. Carter, G.W.H. Cheeseman, Tetrahedron 33 (1977) 827–832.
[13] G.W.H. Cheeseman, J. Chem. Soc. (1962) 1170–1176.
[14] A. Bhat, H.M. Change, L.J. Wallance, D.M. Weinstei, G. Shams, C.C. Garris, R.A. Hill, Bioorgan. Med. Chem. 6 (1998) 271–282.
[15] W.B. Leighton, G.S. Forbes, J. Am. Chem. Soc. 52 (1930) 3139–3152.
[16] D. Avci, J. Nobles, L.J. Mathias, Polymer 44 (2003) 963–968.
[17] A.D. Becke, J. Chem. Phys. 98 (1993) 5648–5652.
[18] C. Lee, W. Yang, R.G. Parr, Phys. Rev. B 37 (1988) 785–789.
[19] M.J. Frisch, G.W. Trucks, H.B. Schlegel, G.E. Scuseria, M.A. Robb, J.R. Cheeseman, J.A. Montgomery Jr., T. Vreven, K.N. Kudin, J.C. Burant, J.M. Millam, S.S. Iyengar, J. Tomasi, V. Barone, B. Mennucci, M. Cossi, G. Scalmani, N. Rega, G.A. Petersson, H. Nakatsuji, M. Hada, M. Ehara, K. Toyota, R. Fukuda, J. Hasegawa, M. Ishida, T. Nakajima, Y. Honda, O. Kitao, H. Nakai, M. Klene, X. Li, J.E. Knox, H.P. Hratchian, J.B. Cross, C. Adamo, J. Jaramillo, R. Gomperts, R.E. Stratmann, O. Yazyev, A.J. Austin, R. Cammi, C. Pomelli, J.W. Ochterski, P.Y. Ayala, K. Morokuma, G.A. Voth, P. Salvador, J.J. Dannenberg, V.G. Zakrzewski, S. Dapprich, A.D. Daniels, M.C. Strain, O. Farkas, D.K. Malick, A.D. Rabuck, K. Raghavachari, J.B. Foresman, J.V. Ortiz, Q. Cui, A.G. Baboul, S. Clifford, J. Cioslowski, B.B. Stefanov, G. Liu, A. Liashenko, P. Piskorz, I. Komaromi, R.L. Martin, D.J. Fox, T. Keith, M.A. Al-Laham, C.Y. Peng, A. Nanayakkara, M. Challacombe, P.M.W. Gill, B. Johnson, W. Chen, M.W. Wong, C. Gonzalez, J.A. Pople, Gaussian 03 Revision B. 01, Gaussian, Inc., Pittsburgh, PA, 2003.
[20] R. Bauernschmitt, R. Ahlrichs, Chem. Phys. Lett. 256 (1996) 454–464.
[21] N. Urasaki, S. Yoshida, T. Ogawa, K. Kozawa, T. Uchida, Bull. Chem. Soc. Jpn. 67 (1994) 2024–2030.
[22] S.A. Alkaitis, G. Beck, M. Graetzel, J. Am. Chem. Soc. 97 (1975) 5723–5729.
[23] D. Rehm, A. Weller, Isr. J. Chem. 8 (1970) 259–271.
[24] D. Dossow, Q.Q. Zhu, G. Hizal, Y. Yagci, W. Schnabel, Polymer 37 (1996) 2821–2826.